

Subcellular Localization and Tumor-suppressive Functions of 15-Lipoxygenase 2 (15-LOX2) and Its Splice Variants*

Received for publication, February 24, 2003, and in revised form, April 11, 2003
Published, JBC Papers in Press, April 18, 2003, DOI 10.1074/jbc.M301920200

Bobby Bhatia^{‡§}, Carlos J. Maldonado^{‡¶}, Shaohua Tang[‡], Dhyan Chandra^{‡||}, Russell D. Klein[‡],
Dharam Chopra^{**}, Scott B. Shappell^{‡‡}, Peiying Yang^{§§}, Robert A. Newman^{§§¶¶},
and Dean G. Tang^{‡|||}

From the [‡]Department of Carcinogenesis, the University of Texas M. D. Anderson Cancer Center, Science Park Research Division, Smithville, Texas 78957, the ^{**}Institute of Chemical Toxicology, Wayne State University, Detroit, Michigan 48226, the ^{‡‡}Department of Pathology, Vanderbilt University School of Medicine, Nashville, Tennessee 37221, and the ^{§§}Department of Experimental Therapeutics, University of Texas M. D. Anderson Cancer Center, Houston, Texas 77030

15-Lipoxygenase 2 (15-LOX2), the most abundant arachidonate (AA)-metabolizing enzyme expressed in adult human prostate, is a negative cell-cycle regulator in normal human prostate epithelial cells. Here we study the subcellular distribution of 15-LOX2 and report its tumor-suppressive functions. Immunocytochemistry and biochemical fractionation reveal that 15-LOX2 is expressed at multiple subcellular locations, including cytoplasm, cytoskeleton, cell-cell border, and nucleus. Surprisingly, the three splice variants of 15-LOX2 we previously cloned, *i.e.* 15-LOX2sv-a/b/c, are mostly excluded from the nucleus. A potential bi-partite nuclear localization signal (NLS), ²⁰³RKGLWRSLSNEMKRIFNFR²²¹, is identified in the N terminus of 15-LOX2, which is retained in all splice variants. Site-directed mutagenesis reveals that this putative NLS is only partially involved in the nuclear import of 15-LOX2. To elucidate the relationship between nuclear localization, enzymatic activity, and tumor suppressive functions, we established PCa cell clones stably expressing 15-LOX2 or 15-LOX2sv-b. The 15-LOX2 clones express 15-LOX2 in the nuclei and possess robust enzymatic activity, whereas 15-LOX2sv-b clones show neither nuclear protein localization nor AA-metabolizing activity. To our surprise, both 15-LOX2- and 15-LOX2sv-b-stable clones proliferate much slower *in vitro* when compared with control clones. More importantly, when orthotopically implanted in nude mouse prostate, both 15-LOX2 and 15-LOX2sv-b suppress PC3 tumor growth *in vivo*. Together, these results suggest that both 15-LOX2 and 15-LOX2sv-b suppress prostate tumor development, and the tumor-suppressive functions apparently do not necessarily depend on AA-metabolizing activity and nuclear localization.

15-Lipoxygenase 2 (15-LOX2)¹ is a recently cloned lipoxygenase that shows the highest homology (~80% amino acid identity) to murine 8-LOX, with ~40% identity to human 5-LOX, 12-LOX, or 15-LOX1 (1). It has at least three splice variants (termed 15-LOX2sv-a/b/c) (2, 3) and metabolizes preferentially arachidonic acid (AA) to 15(S)-hydroxyeicosatetraenoic acid (15(S)-HETE) (1). 15-LOX2 shows an interesting tissue expression pattern, *i.e.* mainly in prostate, lung, skin, and cornea (1–3). This tissue-restricted expression pattern suggests that 15-LOX2 may play a role in the normal development and its abnormal expression/function may contribute to tumorigenesis in these organs. Indeed, work by Shappell *et al.* (4–6) indicates that 15-LOX2 mRNA, protein expression, and enzymatic activity are decreased in high grade prostate intraepithelial neoplasia (PIN) and prostate cancer (PCa), and the expression levels of 15-LOX2 are inversely correlated with the pathological grade (Gleason scores) of the patients. We recently reported that 15-LOX2 is a negative cell-cycle regulator in normal human prostate (NHP) epithelial cells (3). These observations (3–6) together raise the possibility that 15-LOX2 may represent an endogenous prostate tumor suppressor, and its down-regulation may contribute to PCa development. Here we provide experimental data in support of this possibility as restoration of 15-LOX2 expression inhibits PCa cell proliferation *in vitro* and tumor development *in vivo*. We further show that the tumor-suppressive functions of 15-LOX2 do not necessarily depend on the AA-metabolizing activity and nuclear localization as 15-LOX2sv-b, a splice variant that does not metabolize AA and is mostly excluded from nucleus, demonstrates similar inhibitory effect on PCa development.

MATERIALS AND METHODS

Cells and Reagents—Six primary NHP cell strains, NHP1–NHP6, were prepared from six different donors. NHP1, NHP3, NHP4, and NHP6 cells were obtained from Clonetics (Walkersville, MD), and NHP2 and NHP5 cells were generated as previously described (7–9). These cells were cultured in serum-free, PrEBM medium (Clonetics)

* This work was supported in part by NCI, National Institute of Health (NIH) Grant CA-90297, Burroughs-Wellcome Fund Award BWF-1122, Department of Defense Grant DAMD17-03-1-0137, NIEHS, NIH Cancer Center Grant ES07784, and University of Texas M. D. Anderson Cancer Center Institutional fund (to D. G. T.). The costs of publication of this article were defrayed in part by the payment of page charges. This article must therefore be hereby marked “advertisement” in accordance with 18 U.S.C. Section 1734 solely to indicate this fact.

§ A student in the Graduate School of Biomedical Sciences program.

¶ Supported by NIH Post-doctoral Training Grant T32 CA09480-16.

|| Supported by Department of Defense Postdoctoral Traineeship Award DAMD17-02-1-0083.

¶¶ Supported by NCI, NIH Cancer Center Support Grant CA16672.

||| To whom correspondence should be addressed: Dept. of Carcinogenesis, the University of Texas M. D. Anderson Cancer Center, Science Park Research Division, Park Rd. 1C, Smithville, TX 78957. Tel.: 512-237-9575; Fax: 512-237-2475; E-mail: dtang@sprd1.mdacc.tmc.edu.

¹ The abbreviations used are: 15-LOX2, 15-lipoxygenase 2; 15-LOX2sv-a/b/c, 15-lipoxygenase 2 splice variant a, b, or c; AA, arachidonic acid; CAP, cytoskeleton-associated proteins; Cox-II, cytochrome oxidase subunit II; CSK, cytoskeleton; LDH, lactate dehydrogenase; NHP, normal human prostate epithelial cells; PCa, prostate cancer; NLS, nuclear localization signal; PPAR-γ, peroxisome proliferator-activated receptor-γ; WCL, whole cell lysate; DAPI, 4',6-diamidino-2-phenylindole; 15(S)-HETE, 15(S)-hydroxyeicosatetraenoic acid; FBS, fetal bovine serum; GFP, green fluorescent protein; HM, heavy membrane; LM, light membrane; MES, 4-morpholineethanesulfonic acid; hrGFP, humanized *Renilla* GFP; IRES, internal ribosomal entry site; UT, untransfected; UG, urogenital; RT, reverse transcription; ER, endoplasmic reticulum; pCMV, cytomegalovirus promoter.

supplemented with insulin, epidermal growth factor, hydrocortisone, bovine pituitary extract, and cholera toxin, and used during passages 2–6 (3). PCa cell lines, *i.e.* PPC-1, PC3, and LNCaP, were cultured in RPMI 1640 supplemented with 10% heat-inactivated fetal bovine serum (FBS) and antibiotics. HEK 293 cells were purchased from ATCC and cultured in Dulbecco's modified Eagle's medium supplemented with 5% FBS and antibiotics.

Rabbit polyclonal anti-15-LOX2 antibody was described before (4). Rabbit polyclonal anti-E-cadherin and goat polyclonal anti-lamin A antibodies were obtained from Santa Cruz Biotechnology Inc. (Santa Cruz, CA). Monoclonal anti-human vinculin (clone hVIN-1) was bought from Sigma (St. Louis, MO). Goat anti-lactate dehydrogenase (LDH) antibody was purchased from Chemicon (Chemicon International, Inc., Temecula, CA). Monoclonal anti-actin and anti-cytochrome *c* oxidase subunit II (Cox-II) antibodies were purchased from ICN (Indianapolis, IN) and BD Pharmingen (San Diego, CA), respectively. A monoclonal anti-BrdUrd (5-bromo-2'-deoxyuridine) antibody and a rabbit polyclonal anti-Bap31 antibody were kindly provided by Drs. M. Raff and G. Shore, respectively. Anti-GFP (green fluorescent protein) antibodies were obtained from Clontech (Palo Alto, CA). All secondary antibodies (goat anti-mouse or -rabbit IgG or rabbit anti-goat IgG conjugated to horseradish peroxidase, fluorescein isothiocyanate, or Rhodamine) were acquired from Amersham Biosciences (Piscataway, NJ). Liposome FuGENE 6 was bought from Roche Applied Science (Indianapolis, IN). All other chemicals were bought from Sigma unless specified otherwise.

Immunohistochemistry of 15-LOX2 Expression in Tissue Sections—Paraffin-embedded sections of normal prostate tissues and PCa were blocked for endogenous peroxidase activity with 3% H₂O₂ in water for 10 min. Antigen retrieval was done by incubating the slides with 10 mM citrate buffer (pH 6.0) for 10 min in a microwave oven. Slides were then blocked for nonspecific binding in 10% goat whole serum (30 min) followed by incubation in anti-15-LOX2 antibody (30 min, room temperature). Slides were finally incubated with goat anti-rabbit IgG conjugated to horseradish peroxidase followed by substrate (dimethyl amino azobenzene) incubation.

Immunofluorescence Detection of 15-LOX2 Expression in Cultured NHP Cells—The basic procedure was as described previously (3). For double labeling of 15-LOX2 and E-cadherin or 15-LOX2 and vinculin, cells were first labeled for 15-LOX2 followed by goat anti-rabbit IgG conjugated to fluorescein isothiocyanate. After post-blocking in 15% goat whole serum, cells were incubated with antibodies against E-cadherin or vinculin followed by secondary antibody conjugated to Rhodamine.

Western Blotting and Subcellular Fractionation—Whole cell lysate (WCL) was prepared in TNC buffer (10 mM Tris acetate, pH 8.0, 0.5% Nonidet P-40, and 5 mM CaCl₂) or complete radioimmune precipitation assay (RIPA) buffer (50 mM Tris-HCl, pH 7.5, 150 mM NaCl, 1% Nonidet P-40, 0.5% sodium deoxycholate, 0.5% Triton X-100, 10 mM EDTA) containing protease inhibitor mixture. The WCL prepared in TNC generally contains much lower nuclear, cytoskeletal, or cytoskeleton (CSK)-associated organelles (such as mitochondria) or proteins. Protein concentrations were determined by MicroBCA kit (Pierce, Rockford, IL). Samples containing same amounts of proteins were loaded on 15% SDS-PAGE and Western blotting performed using enhanced chemiluminescence (ECL).

Subcellular fractionation was carried out in log-phase NHP6 cells as previously described (10–13) with slight modifications. Briefly, heavy membrane (HM) and light membrane (LM) fractions and cytosol were prepared using homogenization combined with differential centrifugation. Nuclei were prepared using the NUCLEI EZ PREP kit (Sigma). To prepare CSK and CSK-associated proteins (CAP) (10), NHP6 cells were first lysed in TNC buffer by scraping. The Nonidet P-40-insoluble pellet was extracted (10 min, 3×) on ice with high salt, Triton-containing CSK extraction buffer (600 mM KCl, 1.0 mM MgCl₂, 50 mM MES, pH 7.6, 10 μg/ml DNase, 10 μg/ml RNase, 1% Triton X-100, and protease mixture). The Triton-resistant residue was designated as CSK, and the Triton-soluble portions from each extraction were pooled and proteins precipitated with an equal volume of ice-cold acetone (10). The resultant protein pellet was designated CAP (10). 50–100 μg of each subcellular fraction was used in Western blotting for 15-LOX2. Then the same membrane was stripped and reprobed for various marker proteins as detailed in the text.

Establishing Stable PCa Cell Lines Expressing 15-LOX2 or 15-LOX2sv-b—15-LOX2 or 15-LOX2 splice variant cDNAs (3) were subcloned into pIRES-hrGFP (Stratagene, La Jolla, CA), in which the target gene (*i.e.* 15-LOX2 or 15-LOX2sv-a/b/c) is driven by pCMV and hrGFP (humanized *Renilla* green fluorescent protein) is transcribed from an internal ribosomal entry site (IRES). The resultant vectors

were designated p15-LOX2-hrGFP, p15-LOX2sv-a-hrGFP, p15-LOX2sv-b-hrGFP, and p15-LOX2sv-c-hrGFP, respectively. These vectors, along with pIRES-hrGFP empty vector, were first transiently transfected into 293 cells to characterize their expressions. To establish stable clones, PC3 or LNCaP cells were co-transfected with pIRES-hrGFP, p15-LOX2-hrGFP, or p15-LOX2sv-b-hrGFP and pCMV-neo (Invitrogen) as a selectable marker. 48 h after transfection, G418 was added to the medium (800 μg/ml for LNCaP and 1 mg/ml for PC3 cells, respectively). Two weeks later, antibiotic-resistant PC3 cells were harvested and plated at clonal density (*i.e.* 50–100 cells/10-cm dish) and individual GFP-positive clones were selected, under an inverted fluorescence microscope, using a cloning ring. For LNCaP cells, stable clones were established by first enriching GFP-positive cells using fluorescence-activated cell sorting, followed by a limiting dilution method in 96-well culture plates. Two to four stable clones of each cell type were propagated and characterized by both Western blotting and immunofluorescence microscopy.

Determination of 15-HETE Production in Stably Transfected PCa Cells by Liquid Chromatography and Tandem Mass Spectrometry—Untransfected LNCaP or PC3 cells, or these cells stably transfected with pIRES-hrGFP, p15-LOX2-hrGFP, or p15-LOX2sv-b-hrGFP, were used to measure 15(S)-HETE production as previously detailed (3).

Effect of 15-LOX2 Expression on PCa Cell Proliferation—Untransfected PC3 cells or stable PC3 cell transfectants (passage 8) were plated, in quadruplicate, in 24-well flat-bottom culture plates at 5000 cells/well. The cells were cultured in RPMI medium containing 1, 2, or 5% FBS. In some conditions, AA at 1–25 μM was added in the culture medium. 72 h after plating, the numbers of dead and live cells in each well were determined by harvesting both floating and adherent cells and counting using the trypan dye exclusion assays (9). The results were expressed as a percentage of the control, and the experiment was repeated three times.

Effect of 15-LOX2 Expression on PCa Development in Vivo—Surgical orthotopic implantation was carried out to assess the effect of restoration of 15-LOX2 expression on PCa development *in vivo*. The basic procedure was previously described (14). Briefly, animals were anesthetized by intraperitoneal injection of Nembutal Mix (10 μl/g of body weight). Four groups of PC3 cells, *i.e.* untransfected (UT) or cells transfected with pIRES-hrGFP (GFP), p15-LOX2-hrGFP (15-LOX2), or p15-LOX2sv-b-hrGFP (15-LOX2sv-b), all at passage 8, were orthotopically injected into athymic NCr-nu (The Jackson Laboratory, Bar Harbor, ME) nude mouse prostate (2 × 10⁶ in 25 μl of RPMI/prostate). Tumor development was monitored 2 weeks after surgical implantation. About 2 months (*i.e.* 63 days) after implantation, the experiment was terminated, animals were sacrificed, and primary tumors together with the urogenital (UG) organs except bladder were dissected out. Tumor weights (with UG organs) were determined, and prostates from all four groups were used in H-E staining and immunohistochemical analysis.

Nuclear Localization of 15-LOX2 and Its Splice Variants—PC3 or LNCaP cells grown on glass coverslips were either untransfected or transiently transfected with various vectors using FuGENE 6 (3). Cells were fixed 48 h after transfection and then processed for 15-LOX2 staining (3). The distribution of 15-LOX2 in the transfected (*i.e.* GFP⁺) cells was observed under a fluorescence microscope. In some cases, stable transfectants of PC3 and LNCaP cells were used in similar studies. In other experiments, cells were used in subcellular fractionation.

Site-specific Mutagenesis of 15-LOX2 and Nuclear Localization Studies—Site-specific mutagenesis was performed to change the 15-LOX2 R203K204, K214R215, and R220R221 to A203S204, R214S215, and A220S221, respectively, using the QuikChange site-specific mutagenesis system (Stratagene) and p15-LOX2-hrGFP as template. A triple mutant was also made. The successfully mutated sequences were confirmed by restriction digestion and sequencing analysis. These 15-LOX2 mutants, along with 15-LOX2 and 15-LOX2sv-a/b expression constructs, were transiently transfected into PC3 cells, and 48 h later, cells were processed for 15-LOX2 staining.

RT-PCR Analysis of the mRNA Levels 15-LOX2 and Its Splice Variants and Mutants—Log-phase LNCaP cells were transfected with pIRES-hrGFP, p15-LOX2-hrGFP, p15-LOX2sv-a-hrGFP, p15-LOX2sv-b-hrGFP, p15-LOX2sv-c-hrGFP, or four NLS mutants mentioned above. 48 h after transfection, cells were selected by adding G418 (800 μg/ml). Ten days later, these G418-selected LNCaP cells, together with untransfected PC3 cells or PC3 stable clones, were harvested for RT-PCR analysis. Total RNA was isolated with the RNeasy Mini kit (Qiagen), and 0.6 μg of the total RNA was used in RT-PCR analysis using the MasterAmp One-Step RT-PCR kit (Epicenter, Madison, WI). Primers C (5'-ACTACCTCCCAAAGAACTTCCCC-3', forward) and D (5'-

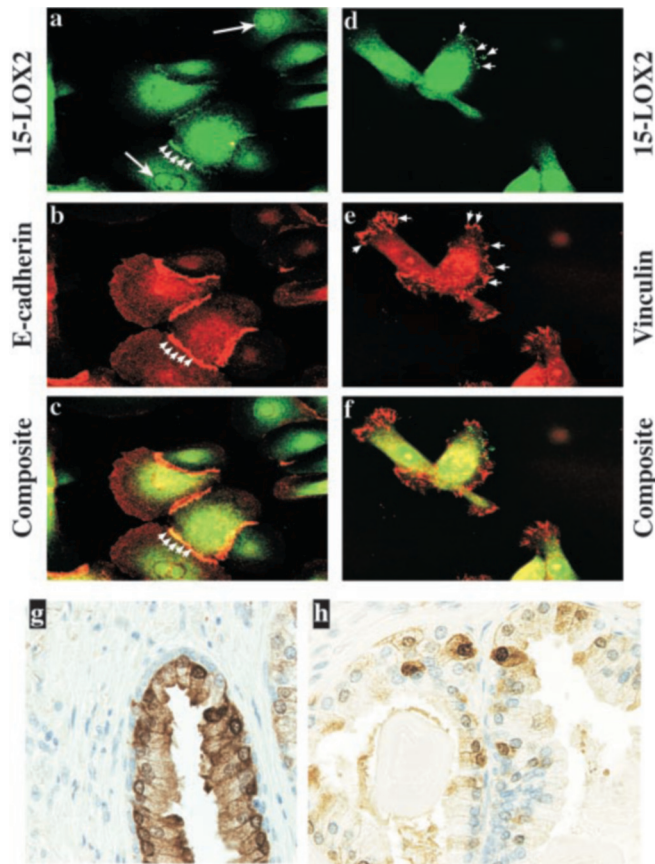


FIG. 1. Immunofluorescent and immunohistochemical analysis of 15-LOX2 expression in NHP cells *in vitro* and benign prostate epithelial cells *in vivo*. *a-f*, NHP2 (P5) grown on glass coverslips were double-labeled with 15-LOX2 and E-cadherin (*a* and *b*, respectively) or with 15-LOX2 and vinculin (*d* and *e*, respectively). *c* and *f* are composite images. *Small arrows* indicate the cell-cell border localization of 15-LOX2, whereas the *large arrows* are the nuclear localization. Note the colocalization of 15-LOX2 with E-cadherin (*a-c*) but not with vinculin (*d-f*). *g* and *h*, prostate tissue sections of normal (*g*) or PIN (*h*) glands stained for 15-LOX2 (brown). Note clear staining at the cell-cell border as well as in the nuclei in addition to cytoplasmic staining in both images. Original magnifications, $\times 400$ for *a-f* and $\times 100$ for *g* and *h*.

TTCAATGCCGATGCCTGTG-3', reverse) were used to amplify 15-LOX2 as previously described (3). This pair of primers amplifies 15-LOX2 and 15-LOX2sv-c as a 546-bp band and 15-LOX2sv-a and 15-LOX2sv-b as a 459-bp band (3). RT-PCR of glyceraldehyde-3-phosphate dehydrogenase was used as a control (3). Plasmids (1 ng) were used as positive controls.

Statistical Analysis—Student's *t* test was used to determine the statistical differences between various experimental groups with $p < 0.05$ considered significantly different.

RESULTS

15-LOX2 Is Expressed in the Nucleus and Other Subcellular Locations—15-LOX2 is a negative cell-cycle regulator in NHP cells (3). In an attempt to understand its molecular mechanisms of action, we studied its subcellular expression in cultured primary NHP cells as well as in benign prostate epithelial cells *in vivo*. As observed previously (3), 15-LOX2 was primarily expressed in the cytoplasm. However, significant amounts of 15-LOX2 were also localized at the cell-cell borders (Fig. 1*a*, *small arrows*) as well as in the nuclei (Fig. 1*a*, *large arrows*). The 15-LOX2 distributed at the cell-cell borders partially co-localized with the adhesion molecule E-cadherin (Fig. 1, *a-c*). In some cells, 15-LOX2 was also observed as discrete dots or clusters at the cell periphery (Fig. 1*d*, *arrows*) resembling cell-matrix interaction sites called focal adhesions (15).

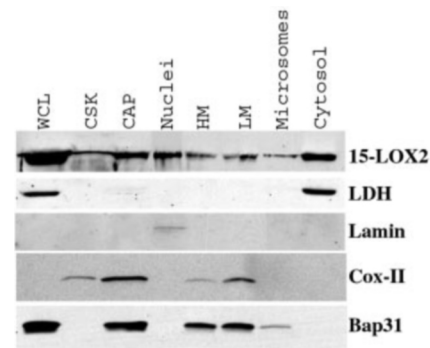


FIG. 2. Analysis of 15-LOX2 expression by subcellular fractionation. NHP 6 (P5) cells were fractionated into CSK, CAP, nuclei, HM, LM, microsomes, and cytosol, as detailed under "Materials and Methods." WCL (prepared in TNC buffer) was used as control. Proteins from each fraction (50 μ g for CSK and microsomes and 100 μ g for all other fractions) were separated on 15% SDS-PAGE and transferred to nitrocellulose membrane. The blot was probed for 15-LOX2 and then for various marker proteins as indicated (see text). *Cox-II*, cytochrome *c* oxidase subunit II; *LDH*, lactate dehydrogenase.

Double staining of 15-LOX2 and vinculin, a protein marker for focal adhesions (15), however, did not reveal any co-localization (Fig. 1, *d-f*). *In vivo*, 15-LOX2 was also expressed in the cytoplasm, cell-cell borders, as well as in the nuclei (Fig. 1*g*). Note that, as previously reported (4), 15-LOX2 was specifically expressed in the glandular prostate epithelial cells *in vivo* but not in basal cells or other cell types including stromal cells (Fig. 1*g*). Also, as noted previously (5), 15-LOX2 staining was reduced in the precursor lesion PIN (prostate intraepithelial neoplasia), and most cells in these lesions homogeneously lost the 15-LOX2 staining (Fig. 1*h*). However, prominent cell membrane and cell-cell border staining, and, in particular, nuclear staining was still evident in some 15-LOX2-positive cells (Fig. 1*h*).

To confirm the subcellular distribution pattern of 15-LOX2 biochemically, we carried out a fractionation analysis (10–13). NHP6 cells were fractionated into CSK, CAP, nuclei, HM (the 1000 $\times g$ pellet containing mainly large mitochondria, plasma membrane sheets, and small amounts of other organelles (13, 16)), LM (the 10,000 $\times g$ pellet containing mainly smaller mitochondria and some lysosomes and peroxisomes (13, 16)), microsomes (*i.e.* the 100,000 $\times g$ pellet containing ER, Golgi, endosomes, and membrane skeleton (12, 16)), and cytosol (*i.e.* the 100,000 $\times g$ supernatant (13)). WCL was used as a control. As shown in Fig. 2, consistent with the immunostaining data (Fig. 1), 15-LOX2 was primarily detected in the cytosol, but significant amounts of 15-LOX2 were also detected in the nuclei and CAP. Lower yet easily detectable levels of 15-LOX2 were also observed in all other fractions, including CSK, HM, LM, and microsomes (Fig. 2). As expected, the highest amount of 15-LOX2 was detected in WCL. The purity of each fraction was confirmed by specific markers. For instance, lactate dehydrogenase (LDH), a cytosolic marker (16), was detected only in the cytosol (Fig. 2), suggesting that there was no contamination of all other subcellular fractions by the cytosol. Similarly, lamin A, a nuclear intermediate filament, was detected only in the nuclei. Cytochrome *c* oxidase subunit II (Cox-II), a mitochondrial inner membrane respiratory complex protein, was detected, as expected, most prominently in CAP and also in CSK (Fig. 2), because most mitochondria normally are associated with microtubules and some other cytoskeletal elements (17). Cox-II was also detected, expectedly, in the HM and LM fractions (Fig. 2), which normally are enriched with the mitochondria (11, 13). Note that no lamin A or Cox-II was detected in WCL, probably due to the low levels of nuclei and mitochondria

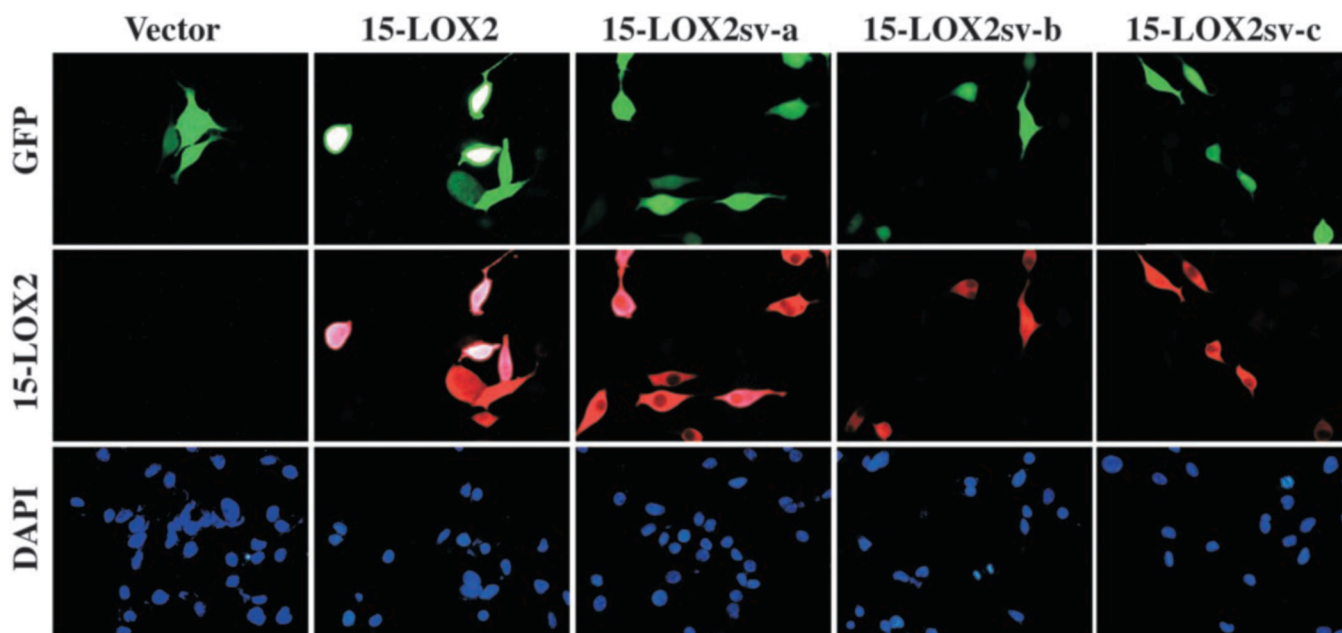


FIG. 3. Lack of nuclear localization of 15-LOX2 splice variants. LNCaP cells were transiently transfected with the vector (*pIRES-hrGFP*), p15-LOX2-IRES-hrGFP (*15-LOX2*), p15-LOX2sv-a-IRES-hrGFP (*15-LOX2sv-a*), p15-LOX2sv-b-IRES-hrGFP (*15-LOX2sv-b*), or p15-LOX2sv-c-IRES-hrGFP (*15-LOX2sv-c*). 48 h post transfection, cells were processed for 15-LOX2 immunostaining and nuclei were counterstained by 4',6-diamidino-2-phenylindole (DAPI). Shown are the representative microphotographs of GFP, 15-LOX2, and DAPI images from three independent experiments with comparable results. Over several thousands of cells analyzed, 15-LOX2 splice variants were clearly excluded from the nucleus in the majority (>95%) of the cells, although the strong transgene expression in some cells tended to mask their non-nuclear expression pattern. Original magnifications, $\times 200$.

in the WCL prepared using the TNC buffer (see "Materials and Methods"). Finally, Bap31, an integral ER membrane protein (18), was detected in CAP, HM, LM, microsomes, and WCL, but not in the cytosol, nuclei, or CSK (Fig. 2).

Collectively, data in Figs. 1 and 2 indicate that, in addition to its predominant expression in the cytosol, 15-LOX2 is also expressed at multiple other subcellular locations, including nuclei, cell-cell borders, CSK, and membrane fractions.

None of the Three 15-LOX2 Splice Variants Is Localized to the Nucleus—The nuclear localization of 15-LOX2 is particularly interesting, because it suggests that the molecule may play a distinct signaling function in the nucleus. Therefore, our subsequent studies focused on the nuclear localization of 15-LOX2 and its relationship with the enzymatic and functional activities. We previously cloned three 15-LOX2 splice variants termed 15-LOX2sv-a/b/c (3). These splice variants have spliced out some critical amino acid residues important for the AA-metabolizing enzymatic activities (2, 3). To determine whether these splice variants are also localized in the nucleus, we transiently transfected various expression plasmids into LNCaP cells, which do not express readily detectable levels of 15-LOX2. As shown in Fig. 3, although 15-LOX2 was distributed throughout the cells, including the nucleus as confirmed by subcellular fractionation (not shown), all three splice variants were mostly excluded from the nucleus. Identical results were observed in stably transfected LNCaP (Fig. 4, *a–d*) or PC3 cells (Fig. 4, *e–h*). It should be pointed out that the obvious lack of nuclear staining of 15-LOX2 splice variants was not due to overall reduced protein expression, because comparable levels of 15-LOX2 and its splice variants were observed in multiple experiments of either transiently (e.g. Fig. 3) or stably (e.g. Fig. 4) transfected PCa cells. A typical example is shown in Fig. 4, in which LNCaP cells stably transfected with 15-LOX2 or 15-LOX2sv-b (Fig. 4, *b* and *d*) or PC3 cells stably transfected with 15-LOX2 or 15-LOX2sv-b (Fig. 4, *f* and *h*) showed very similar levels of protein expression (also see Figs. 5 and 7*b* and the discussion below).

A Putative Nuclear Localization Signal in 15-LOX2 Is Insufficient for Its Nuclear Targeting—Transport between the nucleus and the cytoplasm occurs through the nuclear pore complex on the nuclear envelope, and proteins can enter the nucleus either by diffusion or by signal-mediated transport (19). Generally, only proteins with masses <40 kDa are able to enter the nucleus by passive diffusion (19). Signal-mediated nuclear transport requires energy, optimal temperature, a NLS, and soluble transport machinery (19). Two of the best characterized NLSs are the SV40 large T NLS (often called the classic monopartite NLS), which is composed of a stretch of basic amino acids, and the nucleoplasmin bipartite NLS, which is composed of two basic stretches or clusters separated by 9–12 amino acid residues (19, 20). Recent studies have also revealed other potential NLS (e.g. glycine-rich sequences) that do not conform to these two motifs (19, 20).

Because a significant portion of 15-LOX2 is localized in the nucleus, we reason that there may exist one or more specific NLSs in the molecule responsible for its nuclear targeting. Therefore, we looked for a potential NLS in 15-LOX2 by searching an available data base (cubic.bioc.columbia.edu/predictNLS (20)) and by using tools such as PROSITE and MotifScan. We did not find any credible stretch of basic amino acids that would correspond to the monopartite NLS. However, we did uncover a potential bipartite NLS, ²⁰³RKGLWRS LNEMKRIFNFR²²¹, which is located at the N terminus of 15-LOX2. To determine whether this putative NLS plays a role in the nuclear import of 15-LOX2, we used site-specific mutagenesis to mutate the three di-basic amino acid sequences. As shown in Fig. 5, 15-LOX2 transfected into PC3 cells was localized throughout the cells, including nuclear area (*a–c*), whereas both 15-LOX2sv-a and 15-LOX2sv-b were mostly excluded from nuclei (*d–i*). Compared with 15-LOX2-transfected PC3 cells, cells transfected with the 15-LOX2 mutants, i.e. 15-LOX2RK/AS (Fig. 5, *j–l*), 15-LOX2KR/RS (Fig. 5, *m–o*), 15-LOX2RR/AS (Fig. 5, *p–r*), or triple mutant (not shown), showed partially reduced nuclear staining. Most cells transfected with the 15-LOX2 mutants

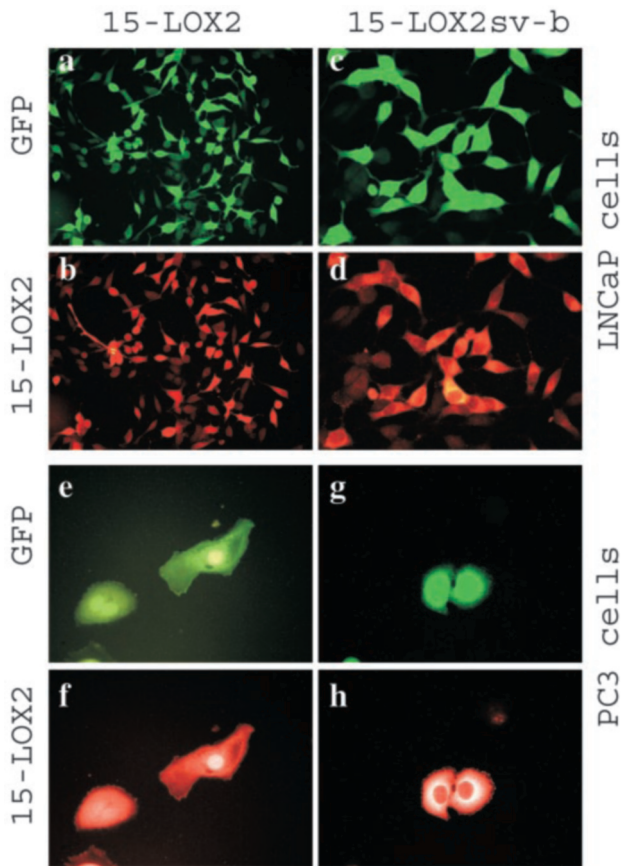


FIG. 4. Nuclear exclusion of 15-LOXsv-b and similar protein levels of 15-LOX2 and 15-LOX2sv-b in stably transfected PCA cells. *a–d*, a clone (clone 1) of LNCaP cells stably transfected with p15-LOX2-hrGFP (*a* and *b*) or p15-LOX2sv-b-hrGFP (*c* and *d*) was plated on glass coverslips and processed for immunofluorescent staining using the rabbit polyclonal anti-15-LOX2 antibody (3). Shown are the representative images of GFP (*a* and *c*) and 15-LOX2 (*b*) or 15-LOX2sv-b (*d*). Note that images in *c* and *d* were enlarged to show the non-nuclear expression pattern of 15-LOX2sv-b. Original magnifications: *a* and *b*, $\times 200$; *c* and *d*, $\times 400$. *e–h*, a clone (clone 1) of PC3 cells stably transfected with p15-LOX2-hrGFP (*e* and *f*) or p15-LOX2sv-b-hrGFP (*g* and *h*) was processed for immunofluorescent staining. Shown are the representative images of GFP (*e* and *g*) and 15-LOX2 (*f*) or 15-LOX2sv-b (*h*). Original magnifications: $\times 400$. Untransfected LNCaP or PC3 cells, or LNCaP or PC3 cells stably transfected with pIRES-hrGFP, showed no 15-LOX2 staining (not shown; also see Fig. 3 and Ref. 3). Note that 15-LOXsv-b is mostly excluded from the nucleus in both LNCaP (*d*) and PC3 (*h*) cells and that similar protein levels of 15-LOX2 and 15-LOX2sv-b were observed in stably transfected PCA cells (compare *d* versus *b* or *h* versus *f*).

showed a nuclear staining intensity between those of 15-LOX2 and 15-LOX2sv-a/b (e.g. Fig. 5, *j*, *m*, and *p*; arrows). These observations suggest that the Arg²⁰³–Arg²²¹ NLS is only partially involved in the nuclear import of 15-LOX2.

Similar to the 15-LOX2 splice variants transfected into PCA cells (Figs. 3 and 4), the 15-LOX2 NLS mutants transfected into PC3 cells also showed levels of protein expression comparable to that of 15-LOX2 on immunofluorescence staining (Fig. 5). Because the transient transfection efficiency varied greatly with different expression constructs and the efficiency (1–10%) generally did not allow us to quantify the protein levels by Western blotting, we adopted a different approach to analyze the mRNA levels of 15-LOX2 and its variants or NLS mutants transfected into PCA cells. For this purpose, LNCaP cells were first transiently transfected with various expression constructs followed by selection with G418 for 10 days. At the end of the selection, the majority of G418-resistant cells were GFP-positive, and these enriched cells were then used in RT-PCR anal-

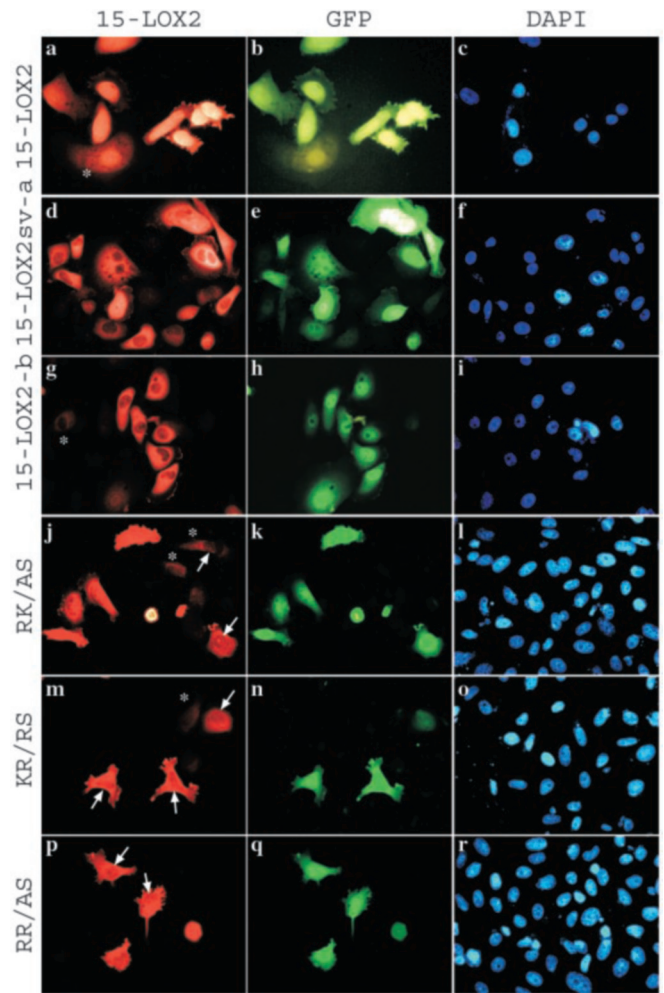


FIG. 5. Partial involvement of the putative NLS (203^{RKGL}–WRSLNEMKRIFNFR²²¹) in the import of 15-LOX2 to the nucleus. The underlined RK, KR, and RR sequences were mutated individually or in combination as described under “Materials and Methods.” The respective expression plasmids, along with 15-LOX2, 15-LOX2sv-a, or 15-LOX2sv-b vectors, were transfected into PC3 cells. Shown are the representative microphotographs of 15-LOX2 (*a*, *d*, *g*, *j*, *m*, and *p*), GFP (*b*, *e*, *h*, *k*, *n*, and *q*), and DAPI (*c*, *f*, *i*, *l*, *o*, and *r*) images. Note that 15-LOX2sv-a (*d*) and 15-LOX2sv-b (*g*) were excluded from the nucleus in most cells, whereas 15-LOX2 was expressed throughout the cell, including the nuclear area (*a*). The RK/AS (*j*), KR/RS (*m*), and RR/AS (*p*) mutants and the triple mutant (not shown) showed reduced nuclear staining (arrows). Asterisks in *a*, *d*, *g*, *j*, and *m* illustrate several transfected 15-LOX2-positive cells that are only weakly positive or negative for GFP, probably because GFP was translated downstream of 15-LOX2 through IRES. The images are representative of the results from two independent experiments. Original magnifications: $\times 200$.

ysis using a pair of primers that could pick up 15-LOX2 and all its three splice variants (3). As shown in Fig. 6, untransfected LNCaP cells and LNCaP cells transfected with pIRES-hrGFP did not express 15-LOX2 or any splice variant, consistent with previous observations (3) as well as with protein data (e.g. Fig. 3). In contrast, LNCaP cells transfected with 15-LOX2 or its splice variants or NLS mutants showed overall similar mRNA levels (Fig. 6; data not shown for 15-LOX2sv-c and the NLS triple mutant). In fact, we consistently observed slightly higher mRNA levels for most 15-LOX2 splice variants or mutants (Fig. 6). These results are consistent with our immunofluorescence data that show similar protein levels of 15-LOX2 and its variants or NLS mutants transfected into the PCA cells.

Restoration of 15-LOX2 Expression Inhibits PCA Cell Proliferation in Vitro and Prostate Tumor Development in Vivo: 15-LOX2sv-b Also Demonstrates Significant Inhibitory Effect—

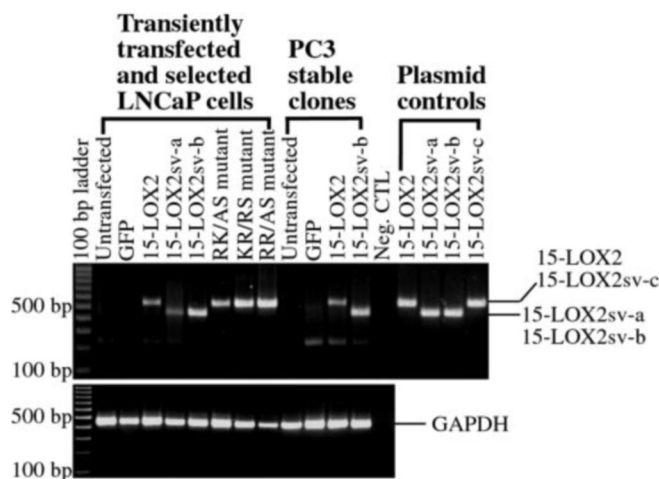


FIG. 6. Similar levels of mRNA expression of 15-LOX2 and its splice variants or NLS mutants transfected into PCa cells. LNCaP cells were transiently transfected with various expression constructs, selected for using G418, and then used for RNA extraction and RT-PCR analysis, as detailed under "Materials and Methods." PC3 stable clones were also analyzed for mRNA expression. The RT-PCR was performed using C-D primers, which amplify 15-LOX2 and 15-LOX2sv-c as a 546-bp band and 15-LOX2sv-a and 15-LOX2sv-b as a 459-bp band (3). RT-PCR of glyceraldehyde-3-phosphate dehydrogenase was used as a control (3). The respective plasmids (the last four lanes; 1 ng each) were used as positive controls.

Most PCa cells demonstrate reduced or lost expression of 15-LOX2 (3–6), suggesting that 15-LOX2 may represent an endogenous prostate tumor suppressor. To directly test this hypothesis, we started by attempting to establish PCa cell lines (PPC-1 and LNCaP) stably expressing 15-LOX2 using the pCMS expression constructs (3), in which 15-LOX2 or its splice variants are driven by the CMV promoter, whereas the EGFP module is driven by the SV40 promoter. Multiple experiments indicated that, although we could initially establish stable clones expressing both 15-LOX2 (or splice variants) and GFP, expression of 15-LOX2 or its splice variants was preferentially lost starting from passage 3 (not shown). These results are consistent with the concept that 15-LOX2, and perhaps its splice variants as well, are inhibitory to PCa cells.

We then made expression constructs in the pIRES-hrGFP vector, in which the transcription of both 15-LOX2 (or splice variants) and hrGFP is controlled by the same CMV promoter and translation of hrGFP is initiated from an internal ribosomal entry site (IRES). When transiently transfected into 293 (not shown) or PCa cells (Figs. 3–6), the expected protein products were detected by immunofluorescence and/or Western blotting. We then used these constructs and established stable PC3 and LNCaP clones expressing 15-LOX2 or 15-LOX2sv-b. Of the several hundred GFP⁺ clones transfected with 15-LOX2 or 15-LOX2sv-b that we screened, only ~1% of the cells could be made into long term stable clones. By contrast, ~60% of GFP⁺ cells transfected with hrGFP alone could become stable clones. These observations are also consistent with the 15-LOX2 being inhibitory to PCa cells.

Shown in Fig. 7a is one clone of PC3 cells expressing 15-LOX2, 15-LOX2sv-b, or GFP alone. Nearly all cells in the clone were GFP-positive but only the cells stably transfected with 15-LOX2 or 15-LOX2sv-b were double positive for 15-LOX2 and GFP (Fig. 7b). Again, 15-LOX2 was expressed in the whole cell, including the nucleus, but 15-LOX2sv-b was mostly excluded from the nucleus as revealed by both immunolabeling (Fig. 7b) and subcellular fractionation (Fig. 7c). Similar results were observed with several other PC3 cells clones as well as with stable LNCaP clones (not shown). Note that in both Western

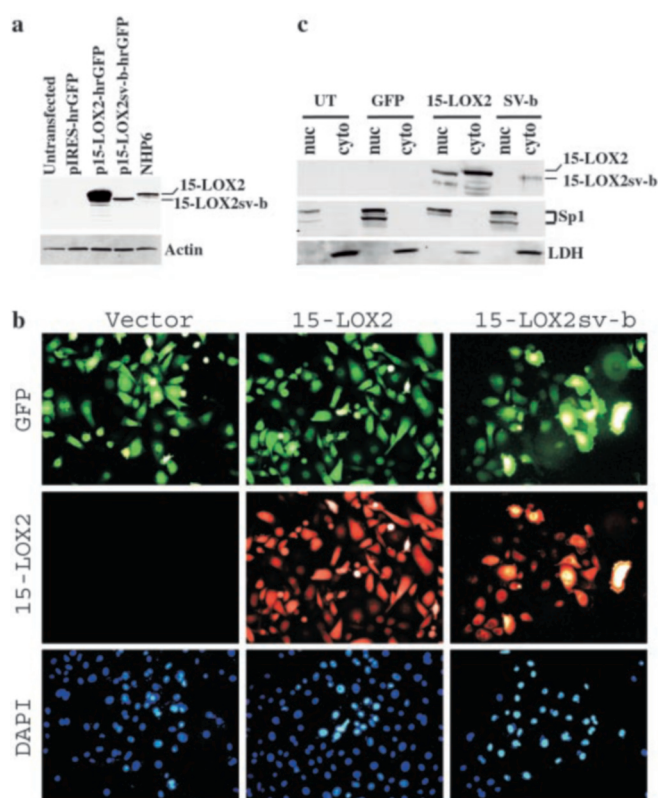


FIG. 7. Establishment of stable PC3 cell clones expressing 15-LOX2 or 15-LOX2sv-b. a, Western blotting of 15-LOX2 and 15-LOX2sv-b in a stable clone of PC3 cells (passage 6) using 30 μ g of whole cell lysate. The 15-LOX2 and 15-LOX2sv-b protein bands were indicated on the right. NHP6 (passage 5) cells were used as a positive control. b, the same clone of PC3 cells (as shown in a) stably transfected with pIRES-hrGFP (Vector), p15-LOX2-IRES-hrGFP (15-LOX2), or p15-LOX2svb-IRES-hrGFP (15-LOX2sv-b), respectively, were stained for 15-LOX2 and nuclei (DAPI). Original magnifications, $\times 200$. c, nuclear localization of 15-LOX2 but not 15-LOX2sv-b in stably transfected PC3 cells. Subcellular fractionation was carried out as described under "Materials and Methods," and 60 μ g of nuclear (nuc) or cytosolic (cyto) proteins/lane was separated on a 15% SDS-PAGE. After transfer, the membrane was probed for 15-LOX2, stripped, and then reprobed for Sp1 proteins (as a nuclear marker; the upper bands being the phosphorylated Sp1) or LDH. Note that several lower bands were consistently detected in both cytosolic and nuclear fractions from the cells transfected with 15-LOX2, which might be degradation products.

blotting (Fig. 7a) and subcellular fractionation (Fig. 7c), we observed lower protein levels of 15-LOX2sv-b than 15-LOX2. Similar differences were also observed in transiently transfected 293 cells (3) as well as in other stable clones of PC3 and LNCaP cells (not shown). This difference was unlikely due to differential protein expression as we consistently observed, on immunofluorescence microscopy, very similar protein levels of 15-LOX2 and its splice variants or NLS mutants (Figs. 3–5 and 7b). More importantly, we observed similar levels of 15-LOX2 and 15-LOX2sv-b mRNA in the stably transfected PC3 cells (Fig. 6). These observations, together, suggest that the polyclonal anti-15-LOX2 antibody preferentially recognizes 15-LOX2 and does not recognize its splice variants well on Western blotting (e.g. Fig. 7, a and c), although it recognizes equally well the undenatured proteins of 15-LOX2 and its variants or NLS mutants in immunofluorescent staining (e.g. Figs. 3–5, and 7b). This conclusion is also supported by our multiple experiments with transiently transfected 293 cells as well as with other PCa stable clones (3; data not shown). We are currently developing 15-LOX2 isoform-specific antibodies to directly address this issue.

As expected, untransfected PC3 and LNCaP cells, as well as

TABLE I
15(S)-HETE production in stably transfected PCa cells

15(S)-HETE production was measured in lysates from log-phase cells, in the presence of exogenous AA (100 μ M; 37 °C \times 10 min) using LC/MS/MS analysis as previously described (3). Data were obtained from two separate experiments and the values are mean \pm S.D. derived from two to three samples with each cell type.

Cells	15(S)-HETE level ng/10 ⁶ cells
PC3	
Untransfected	0.63 \pm 0.18
GFP	1.33 \pm 0.15
15-LOX2	27.95 \pm 3.16 ^a
15-LOX2sv-b	1.77 \pm 0.23
LNCaP	
Untransfected	0.85 \pm 0.02
GFP	0.73 \pm 0.05
15-LOX2	13.42 \pm 0.25 ^a
15-LOX2 ^b	0.024 \pm 0.002
15-LOX2sv-b	0.84 \pm 0.06

^a $p < 0.001$ (Student *t* test).

^b 15(S)-HETE measurement in the absence of exogenous AA.

PC3 and LNCaP cells, transfected with GFP vector alone produced little 15(S)-HETE (Table I), because they do not express appreciable 15-LOX2 (3). By contrast, cells transfected with 15-LOX2 produced a significant amount of 15(S)-HETE (Table I). In contrast to 15-LOX2-transfected cells, cells transfected with 15-LOX2sv-b, in which two exons have been spliced out (3), produced little 15(S)-HETE (Table I). These measurements were done in the presence of added substrate, AA. In the absence of exogenous AA, the 15-LOX2-transfected LNCaP stable clones produced no 15(S)-HETE (Table I), suggesting that there was very little free AA in the cells under the normal culture conditions. Collectively, these data suggest that the 15-LOX2 in the stably transfected PCa cells is enzymatically active (*i.e.* capable of metabolizing AA), whereas the 15-LOX2sv-b is not.

To assess the effect of 15-LOX2 re-expression on PCa development, we first performed a cell proliferation assay using the stable clones. Consistent with our previous transient transfection experiments (3), PC3 cells stably expressing 15-LOX2 expression proliferated slower than either untransfected cells or the vector-transfected cells (Fig. 8*a*). Surprisingly, PC3 cells stably expressing 15-LOX2sv-b, which does not possess AA-metabolizing activity and is mostly excluded from the nucleus (see above), also showed slower cell proliferation (Fig. 8*a*). The inhibitory effect of 15-LOX2 and 15-LOX2sv-b was observed in either 1% or 5% FBS (Fig. 8*a*). As previously observed (3), re-expression of 15-LOX2 or 15-LOX2sv-b by itself did not affect apoptosis in the transfected cells, which were all healthy (*e.g.* Figs. 3–6, and 7*b*). However, in the presence of exogenous AA, the 15-LOX2 stable clones, but not 15-LOX2sv-b clones, showed a significant increase in apoptosis (not shown). For example, in the presence of 5 μ M AA (72 h), only 14% of the PC3 cells stably transfected with 15-LOX2 were alive, compared with 88%, 70%, and 65% survivability in untransfected and PC3 cells stably transfected with GFP or 15-LOX2sv-b, respectively. These results, consistent with previous observations that high doses of 15(S)-HETE induce cell death in PCa cells (3, 21), suggest that the exogenously added AA is metabolized by transfected 15-LOX2 but not 15-LOX2sv-b to produce 15(S)-HETE, which in turn induces cell death.

Next, we carried out an orthotopic tumor implantation experiment in which PC3 cells stably expressing 15-LOX2 or 15-LOX2sv-b or the vector alone were injected into the mouse prostate. The experiment was terminated 63 days post tumor cell inoculation. As shown in Fig. 8 (*b* and *c*), the PC3 tumors

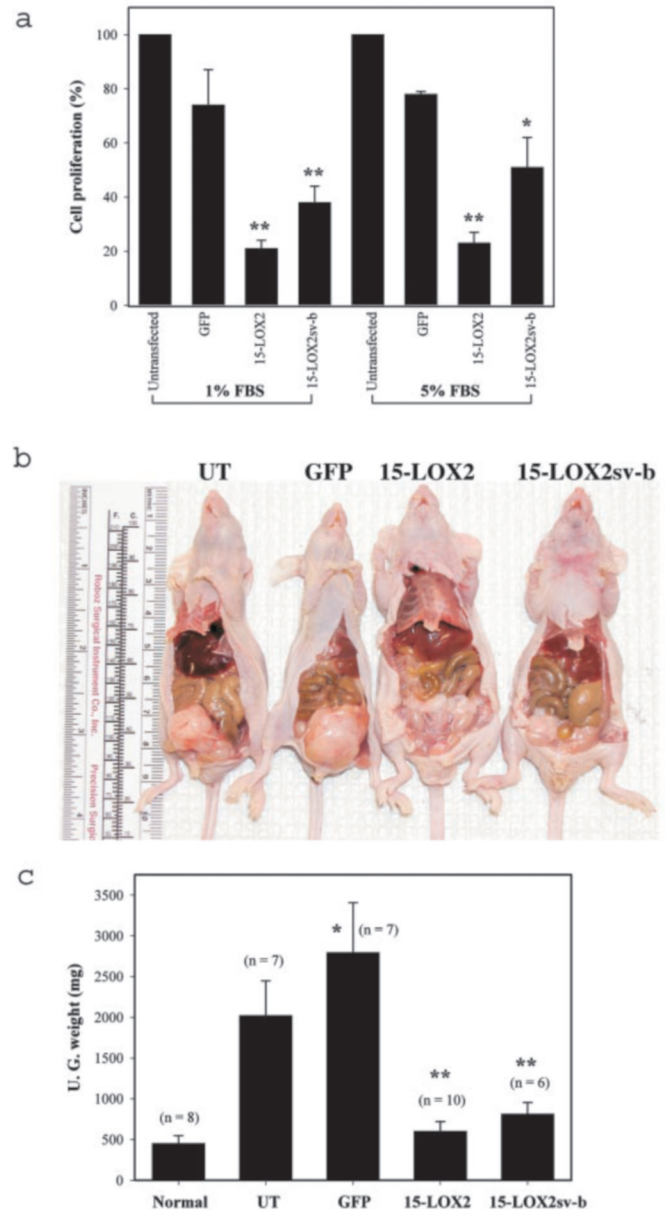


FIG. 8. Inhibition of PC3 cell proliferation *in vitro* (a) and tumor development *in vivo* (b and c) by restoration of 15-LOX2 expression. In *a*, proliferation of untransfected PC3 cells 72 h after plating was used as the baseline and considered 100%. Proliferation of PC3 cells stably transfected with pIRES-hrGFP (GFP), p15-LOX2-IRES-hrGFP (15-LOX2), or p15-LOX2sv-b-IRES-hrGFP (15-LOX2sv-b) was presented as percent proliferation of the untransfected PC3 cells. The bars represent the mean \pm S.D. derived from three independent experiments. *, $p < 0.01$; **, $p < 0.001$. Note that the GFP-transfected stable PC3 cells also proliferated slightly slower (statistically insignificant) than the untransfected controls, as previously observed (3). In *b*, large solid tumors can be easily seen in the UT (untransfected) and GFP groups, whereas the 15-LOX2 and 15-LOX2sv-b groups showed minimal tumor burden. In *c*, the UG (urogenital) weights in the UT and GFP groups are significantly higher ($p < 0.001$) than the uninjected prostates (normal). For unknown reasons, tumors in the GFP group are larger than those in the UT group (*, $p < 0.05$; also see *b*). In contrast, tumors in both the 15-LOX2 and 15-LOX2sv-b groups are significantly (**, $p < 0.001$) smaller than tumors in either the UT or GFP group. The numbers (*n*) of animals in each group are indicated in the parentheses.

bearing 15-LOX2 were significantly smaller than the tumors bearing empty vector (*i.e.* GFP), suggesting that 15-LOX2 re-expression suppresses orthotopically implanted prostate tumor growth *in vivo*. Surprisingly and in support of the *in vitro* data (Fig. 8*a*), the PC3 tumors stably expressing 15-LOX2sv-b were

also significantly smaller than the control tumors (Fig. 8, *b* and *c*). These results together indicate that restored expression of 15-LOX2 inhibits PCa cell proliferation *in vitro* and tumor development *in vivo* by functioning as a negative cell-cycle regulator. Like 15-LOX2, 15-LOX2sv-b also exhibits inhibitory effects.

DISCUSSION

The present study has made the following novel findings: 1) 15-LOX2 is expressed at multiple subcellular locations, including the cell-cell border and nucleus in addition to cytosol; 2) none of the three 15-LOX2 splice variants is expressed in the nucleus; 3) a putative NLS found in the N terminus of 15-LOX2 is partially involved in its nuclear targeting; 4) stable restoration of 15-LOX2 expression in PCa cells inhibits their proliferation *in vitro* and tumor development *in vivo*; and 5) 15-LOX2sv-b, which does not possess the AA-metabolizing activity and is mostly excluded from the nucleus, demonstrates similar inhibitory effects when overexpressed.

Localization of 15-LOX2 at the Cell-Cell Borders—A portion of 15-LOX2 is concentrated at the cell-cell borders in NHP cells *in vitro* as well as in prostate epithelial cells *in vivo* (Fig. 1). Located at the cell-cell borders are cell junctions, including occluding, anchoring, and communicating junctions (22). The anchoring junctions at the cell-cell borders mainly have two types: adherens junctions and desmosomes, both of which hold cells together and are formed by transmembrane adhesion proteins that belong to the cadherin family (22, 23). In adherens junctions, the cytoplasmic tails of cadherins (mainly E-cadherin) bind to anchor proteins (catenins, α -actinin, and vinculin) that tie them to actin filaments (22, 23). In desmosomes, the cytoplasmic tails of cadherins (desmoglein and desmocollin) bind to anchor proteins (plakoglobin and desmoplakin) that tie them to intermediate filaments keratins (22, 23). Interestingly, 15-LOX2 expressed at the cell-cell borders co-localizes with E-cadherin (Fig. 1), the major cadherin molecule expressed in epithelial cells. Western blotting analysis suggests that the 15-LOX2 expression pattern in multiple NHP strains and PCa cell lines coincides with that of a novel E-cadherin splice isoform: both are abundantly expressed in all primary strains and both are lost in all PCa cell lines examined (3).² Subcellular fractionation studies indicate that a significant portion of 15-LOX2 localizes to the CAP as well as the cytoskeleton and membrane fractions (Fig. 2). Together, these observations suggest that some 15-LOX2 molecules are probably associated with the E-cadherin-based adherens junctional structures that help maintain the prostate epithelial integrity. A provocative piece of evidence that supports this possibility is that both 15-LOX2 and E-cadherin are down-regulated or lost in PCa cells, and, in both cases, the loss of 15-LOX2 or E-cadherin expression is inversely correlated with grades and stages of the disease (4, 5, 24, 25).

Several other mammalian LOXs have also been shown to be localized in non-cytosolic compartments and interact with some of their constituents. For example, 5-LOX has been reported to bind actin and α -actinin (26). Platelet-type 12-LOX has been shown to be distributed in the membrane fractions (27) and may interact with some cytoskeletal proteins such as keratin and lamin (28). Finally, 15-LOX1 is well known to interact with, oxidize, and degrade intracellular organelle (*e.g.* ER and mitochondria) membranes (29, 30). These observations together suggest that LOX in general and 15-LOX2 in particular are localized at multiple subcellular microdomains and may participate in distinct cellular processes.

Nuclear Localization of 15-LOX2—Another particularly in-

teresting subcellular localization of 15-LOX2 is in the nucleus. Conceptually, this might provide an explanation to a conundrum we briefly touched upon before (3): how may 15-LOX2 inhibit cell-cycle progression? The main 15-LOX2 metabolite, 15(S)-HETE, has been shown to be a ligand for peroxisome proliferator-activated receptor γ or PPAR γ (21, 31, 32), which has recently been shown to mediate cell-cycle arrest in a diverse array of cell types by suppressing cyclin D1 expression (33–35). Therefore, it is possible that 15-LOX2 may affect cell-cycle arrest in NHP cells (3) by activating PPAR γ . However, the concentration of 15(S)-HETE required to activate PPAR γ is generally $\geq 30 \mu\text{M}$ (21, 31, 32), which may be difficult to attain intracellularly. Therefore, the nuclear localization of 15-LOX2 may allow the generation of sufficient concentrations of the 15(S)-HETE ligand in the proximity of PPAR γ to achieve activation of the receptor.

How is 15-LOX2 imported to the nucleus? A database search allowed us to identify a potential bipartite NLS at the N terminus of 15-LOX2. Site-specific mutagenesis studies reveal that this sequence is only partially involved in the nuclear import of 15-LOX2, because its mutations do not completely eliminate the nuclear expression of the molecule. This result is not surprising because many of these putative NLSs are not the sole determinants of or may even not be involved at all in protein nuclear import (36). The relevant example is 5-LOX, which translocates to the nucleus upon cell stimulation. Several groups identified a typical bipartite NLS (⁶³⁸RKNLEAIVS-VIAERNKKK⁶⁵⁵) that appears to be sufficient for 5-LOX nuclear localization (37–40), whereas another group found that the nuclear import of 5-LOX is probably mediated by a non-conventional signal located in the N-terminal β -barrel domain (41, 42). However, a recent study (43), using more rigorous structural and functional criteria, convincingly demonstrated that neither of these two sequences functions as the true NLS for 5-LOX. It turns out that most of the site-specific mutations (*e.g.* R651Q) carried out in these regions that eliminate the 5-LOX nuclear localization also abrogate the enzymatic activity of the protein, which seems to be important for the nuclear import (43). Instead, a previously unrecognized basic region, ⁵¹⁸RGRKSSGF⁵³⁰PKSVK⁵³⁰ located on a random coil of the catalytic domain, appears to function as the authentic NLS, because this sequence is sufficient to drive GFP to the nucleus and mutations of the underlined basic amino acids significantly diminish the nuclear import of 5-LOX without affecting the enzymatic activity (43). A homology search did not identify related sequence(s) in 15-LOX2. Therefore, it is still unclear how 15-LOX2 is imported into the nucleus. Perhaps the Arg²⁰³–Arg²²¹ NLS in 15-LOX2 cooperates with some other sequences or motifs to import the molecule to the nucleus.

Consistent with the notion that the Arg²⁰³–Arg²²¹ NLS is not the sole determinant of the 15-LOX2 nuclear localization, the three 15-LOX2 splice variants, which all retain this NLS, are mostly excluded from the nucleus. Because these splice variants do not share conserved regions in the sequences divergent from the parental 15-LOX2 (3), it is unlikely that their inability to go into the nucleus is due to deletion of an NLS in these variant-unique regions. The nuclear exclusion of these 15-LOX2 splice variants is also unlikely due to an overall reduced protein expression, because we have consistently observed similar mRNA (Fig. 6) as well as comparable protein expression levels (Figs. 3–5, and 7*b*) of 15-LOX2 and its variants or NLS mutants. It is possible that changes in protein folding or conformation somehow mask the responsible NLS and preclude these splice variants from interacting with importins, proteins required for nuclear import (19), and thus prevent their import. In support of this possibility, we have consistently noticed that

² B. Bhatia and S. Tang, unpublished observations.

the anti-15-LOX2 antibody does not recognize well the denatured 15-LOX2 splice variants on Western blotting (Fig. 7, *a* and *c*; data not shown), suggesting that 15-LOX2 splice variants probably adopt different conformations from 15-LOX2. Alternatively, the reduced or lost enzymatic activity (*i.e.* to metabolize AA to produce 15(*S*)-HETE) renders these variants cytoplasmic, because it has been previously demonstrated that mutations that eliminate the 5-LOX enzymatic activity also abolish its nuclear import (see discussion above). Indeed, compared with 15-LOX2, 15-LOX2sv-a has decreased specificity and activity (2), whereas 15-LOX2sv-b is inactive (Table I). 15-LOX2sv-c is also predicted to be enzymatically dead, because this splice variant lacks the C-terminal isoleucine, which is conserved in all known LOXs and is required for the coordination of catalytic iron (44). Yet another possibility is that 15-LOX2, upon entering the nucleus, is retained in the organelle by physically interacting with one or more other proteins. The 15-LOX2 splice variants, on the other hand, due to structural changes, cannot be retained in the nucleus, although they might be able to be imported. We are currently exploring these possibilities.

15-LOX2sv-b Also Inhibits PCa Cell Proliferation and Tumor Development *in Vivo*—15-LOX2 is a negative cell-cycle regulator (3) and its expression is down-regulated or lost in PCa cells (3–6), suggesting that it may represent an endogenous prostate tumor suppressor. To lend direct support to this possibility, stable re-expression of 15-LOX2 in PCa cells inhibits their proliferation *in vitro* as well as tumor growth *in vivo*. Surprisingly, 15-LOX2sv-b, a splice variant that does not localize in the nucleus and does not possess AA-metabolizing enzymatic activity, also inhibits PCa cell proliferation and tumor growth. This observation is slightly different from our previous transient transfection experiments in which we found apparent but statistically insignificant inhibitory effect of 15-LOX2sv-b on PCa cell proliferation (3). A likely explanation for this discrepancy is that the inhibitory effect of 15-LOX2sv-b is manifested more slowly than that of 15-LOX2 so that by 48 h after transfection only a small inhibitory effect was observed for 15-LOX2sv-b (3). Therefore, the inhibitory effect of 15-LOX2sv-b is fully manifested in the stable clones (this study). Another possibility is that, in previous transient transfection experiments, we used the pCMS expression constructs in which 15-LOX2sv-b and GFP were driven by separate promoters (3). As pointed out under “Results,” in some cells transfected with the pCMS expression constructs the 15-LOX2sv-b (and 15-LOX2) expression is preferentially lost, which may lead to an underestimation of their inhibitory effect on PCa cell proliferation. On the other hand, a tumor-suppressive function of 15-LOX2sv-b is consistent with our previous findings that the mRNA and protein levels of 15-LOX2 splice variants are also reduced in multiple PCa cells (3). The precise biological roles of 15-LOX2 as well as various 15-LOX2 splice variants, the latter of which are also expressed *in vivo*,³ in maintaining physiological prostate homeostasis and in PCa development remain to be clarified. Nevertheless, the results presented in this study raise the possibility that 15-LOX2 may possess biological activities independent of AA-metabolizing activity and independent of its nuclear localization. How 15-LOX2 inhibits PCa cell proliferation without resorting to AA metabolism is currently unclear. One possibility is that 15-LOX2 as well as its splice variants might directly catalyze the oxidation and degradation of biomembranes, analogous to 15-LOX1 (29, 30).

Together, the data presented herein suggest at least two signaling pathways that could conceptually mediate the biolog-

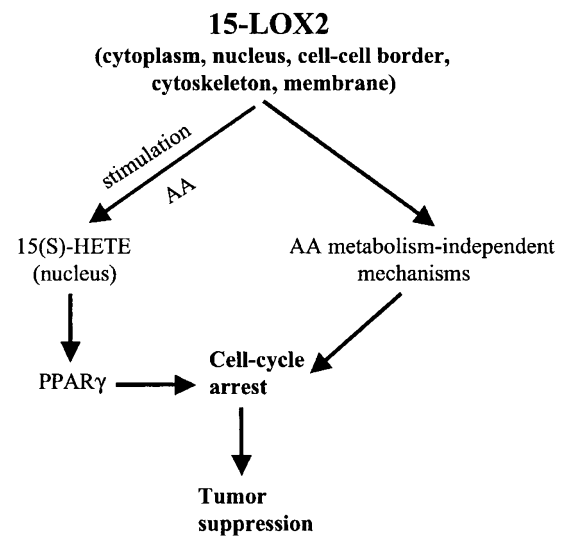


FIG. 9. A hypothetical model of the mechanisms of action of 15-LOX2. See text for details.

ical functions of 15-LOX2 (Fig. 9). Under physiological, unstimulated conditions, 15-LOX2 as well as its splice variants may inhibit cell proliferation through as-yet-unknown mechanisms independent of the nuclear localization and enzymatic activity (*i.e.* AA metabolism). Furthermore, localization of 15-LOX2 to the cell-cell borders and its association with the cytoskeleton may help maintain the differentiated phenotype of prostate glands. Under stimulated conditions, AA will be mobilized resulting in increased 15(*S*)-HETE production in the cells, especially in the nucleus, which may lead to PPAR γ -dependent cell-cycle arrest. This model explains why PCa cells suppress the expression of both 15-LOX2 and its enzymatically inactive splice variants (3). The model also predicts that restoration of 15-LOX2 or its splice variant expression should suppress PCa development, a prediction borne out by orthotopic tumor implantation analysis (Fig. 8).

Acknowledgments—We gratefully acknowledge M. Raff for anti-bromodeoxyuridine antibody, G. Shore for anti-Bap31 antibody, and the Histology Core for help with immunohistochemistry.

REFERENCES

- Brash, A. R., Boeglin, W. E., and Chang, M. S. (1997) *Proc. Natl. Acad. Sci. U. S. A.* **94**, 6148–6152
- Kilty, I., Alison, L., and Vickers, P. J. (1999) *Eur. J. Biochem.* **266**, 83–93
- Tang, S., Bhatia, B., Maldonado, C., Yang, P., Newman, R. A., Liu, J., Chandra, D., Traag, J., Klein, R. D., Fischer, S. M., Chopra, D., Shen, J., Zhou, H., Chung, L. W. K., and Tang, D. G. (2002) *J. Biol. Chem.* **277**, 16189–16201
- Shappell, S. B., Boeglin, W. E., Olson, S. J., Kasper, S., and Brash, A. R. (1999) *Am. J. Pathol.* **155**, 235–245
- Jack, G. S., Brash, A. R., Olson, S. J., Manning, S., Coffey, C. S., Smith, J. A., Jr., and Shappell, S. B. (2000) *Hum. Pathol.* **31**, 1146–1154
- Shappell, S. B., Manning, S., Boeglin, W. E., Guan, Y. F., Roberts, R. L., Davis, L., Olson, S. J., Jack, G. S., Coffey, C. S., Wheeler, T. M., Breyer, M. D., Brash, A. R. (2001) *Neoplasia* **3**, 287–303
- Chopra, D. P., Grignon, D. J., Joikim, A., Mathieu, P. A., Mohamed, A., Sakr, W. A., Powell, I. J., and Sarkar, F. H. (1996) *J. Cell. Physiol.* **169**, 269–280
- Chopra, D. P., Sarkar, F. H., Grignon, D. J., Sakr, W. A., Mohamed, A., and Waghay, A. (1997) *Cancer Res.* **57**, 3688–3692
- Tang, D. G., Li, L., Chopra, D., and Porter, A. T. (1998) *Cancer Res.* **58**, 3466–3479
- Tang, D. G., Timar, J., Grossi, I. M., Renaud, C., Kimler, V., Diglio, C. A., Taylor, J. D., Honn, K. V. (1993) *Exp. Cell Res.* **207**, 361–375
- Joshi, B., Li, L., Taffe, B. G., Zhu, Z., Ben-Josef, B., Taylor, J. D., Porter, A. T., and Tang, D. G. (1999) *Cancer Res.* **59**, 4343–4355
- Liu, J.-W., Chandra, D., Tang, S.-H., Chopra, D., and Tang, D. G. (2002) *Cancer Res.* **62**, 2976–2981
- Chandra, D., Liu, J.-W., and Tang, D. G. (2002) *J. Biol. Chem.* **277**, 50842–50854
- Li, L., Zhu, Z., Joshi, B., Zhang, C., Johnson, C. R., Marnett, L. J., Honn, K. V., Crissman, J. D., Porter, A. T., and Tang, D. G. (1999) *Anticancer Res.* **19**, 61–70
- Tang, D. G., Chen, Y., Diglio, C. A., and Honn, K. V. (1993) *J. Cell Biol.* **121**, 689–704

³ S. B. Shappell, unpublished observations.

16. Evans, W. H. (1992) in *Preparative Centrifugation: A Practical Approach* (Rickwood, D., ed) pp. 233–270, The IRL Press, Oxford, UK
17. Scheffler, I. E. (1999) *Mitochondria*, Wiley-Liss, New York, pp. 26–33
18. Breckenridge, D. G., Nguyen, M., Kuppig, S., Reth, M., and Shore, G. C. (2002) *Proc. Natl. Acad. Sci. U. S. A.* **99**, 4331–4336
19. Kaffman, A., and O'Shea, E. (1999) *Annu. Rev. Cell Dev. Biol.* **15**, 291–339
20. Cokol, M., Nair, R., and Rost, B. (2000) *EMBO Rep.* **1**, 411–415
21. Shappell, S. B., Gupta, R. A., Manning, S., Whitehead, R., Boeglin, W. E., Schneider, C., Case, T., Price, J., Jack, G. S., Wheeler, T. M., Matusik, R. J., Brash, A. R., and DuBois, R. N. (2001) *Cancer Res.* **61**, 497–503
22. Alberts, B., Johnson, A., Lewis, J., Raff, M., Roberts, K., and Walter, P. (2002) *Molecular Biology of the Cell*, 4th Ed., pp. 1065–1090, Garland Science, Taylor & Francis Group, New York
23. Takeichi, M. (1991) *Science* **251**, 1451–1455
24. Umbas, R., Schalken, J. A., Aalders, T. W., Karthaus, H. F., Schaafsman, H. E., Debruyne, F. M., and Isaacs, W. B. (1992) *Cancer Res.* **52**, 5104–5109
25. Bussemakers, M. J., Van Bokhoven, A., Tomita, K., Jansen, C. F., and Schalken, J. A. (2000) *Int. J. Cancer* **85**, 446–450
26. Lepley, R. A., and Fitzpatrick, F. A. (1984) *J. Biol. Chem.* **269**, 24163–24168
27. Timar, J., Raso, E., Dome, B., Li, L., Grignon, D., Nie, D., Honn, K. V., and Hagmann, W. (2000) *Int. J. Cancer* **87**, 37–43
28. Tang, K., Finley, R. L., Jr., Nie, D., and Honn, K. V. (2000) *Biochemistry* **39**, 3185–3191
29. Kuhn, H., and Borngreber, S. (1999) *Adv. Exp. Med. Biol.* **447**, 5–28
30. Walther, M., Anton, M., Wiedmann, M., Fletterick, R., and Kuhn, H. (2002) *J. Biol. Chem.* **277**, 27360–27366
31. Kersten, S., Desvergne, B., and Wahli, W. (2000) *Nature* **405**, 421–424
32. Huang, J. T., Welch, J. S., Ricote, M., Binder, C. J., Wilson, T. M., Kelly, C., Witztum, J. L., Funk, C. D., Conrad, D., and Glass, C. K. (1999) *Nature* **400**, 378–382
33. Wang, C., Fu, M., D'Amico, M., Albanese, C., Zhou, J.-N., Brownlee, M., Lisanti, M. P., Chatterjee, V. K. K., Lazar, M. A., and Pestell, R. G. (2001) *Mol. Cell. Biol.* **21**, 3057–3070
34. Wakino, S., Kintscher, U., Kim, S., Yin, F., Hsueh, W. A., and Law, R. E. (2000) *J. Biol. Chem.* **275**, 22435–22441
35. Kitamura, S., Miyazaki, Y., Hiraoka, S., Nagasawa, Y., Toyota, M., Takakra, R., Kiyohara, T., Shinomura, Y., and Matsuzawa, Y. (2001) *Int. J. Cancer* **94**, 335–342
36. Dingwall, C., and Laskey, R. A. (1991) *Trends Biochem. Sci.* **16**, 478–481
37. Lepley, R. A., and Fitzpatrick, F. A. (1998) *Arch. Biochem. Biophys.* **356**, 71–76
38. Healy, A. M., Peters-Golden, M., Yao, J. P., and Brock, T. G. (1999) *J. Biol. Chem.* **274**, 29812–29818
39. Hanaka, H., Shimizu, T., and Izumi, T. (2002) *Biochem. J.* **361**, 505–514
40. Christmas, P., Fox, J. W., Ursino, S. R., and Soberman, R. J. (1999) *J. Biol. Chem.* **274**, 25594–25598
41. Chen, X. S., Zhang, Y.-Y., and Funk, C. D. (1998) *J. Biol. Chem.* **273**, 31237–31244
42. Chen, X.-S., and Funk, C. D. (2001) *J. Biol. Chem.* **276**, 811–818
43. Jones, S. M., Luo, M., Healy, A. M., Peters-Golden, M., and Brock, T. G. (2002) *J. Biol. Chem.* **277**, 38550–38556
44. Brash, A. R. (1999) *J. Biol. Chem.* **274**, 23679–23682